# Nickel Complexes Based on Molybdopterin-like Dithiolenes: Catalysts for CO 2 Electroreduction

Thibault Fogeron, Pascal Retailleau, Maria Gomez-Mingot, Yun Li, Marc Fontecave

# Nickel complexes based on molybdopterin-like dithiolenes : catalysts for $CO_2$ electroreduction

Thibault Fogeron[a], Pascal Retailleau[b], Maria Gomez-Mingot[a], Yun Li[a]*, Marc Fontecave[a]*

[a]Laboratoire de Chimie des Processus Biologiques, UMR 8229 CNRS, Collège de France, Sorbonne Université, 11 Place Marcelin Berthelot, 75231 Paris Cedex 05, France. E-mail: yun.xu-li@college-de-france.fr; marc.fontecave@college-de-france.fr

[b]Institut de Chimie des Substances Naturelles, CNRS UPR 2301, Université Paris-Saclay, 1, Av. de la Terrasse, 91198 Gif-sur-Yvette, France.

## Abstract

Molecular metal(M)-dithiolene complexes are mimics of the active sites of metalloenzymes such as formate dehydrogenases and CO-dehydrogenases. Recently, the first M-dithiolene (M = Ni) complex behaving as a catalyst for carbon dioxide electroduction has been reported. Here, using dithiolene ligands structurally similar to molybdopterin, new stable Ni-dithiolene complexes have been prepared and characterized. They all catalyze the electroreduction of $CO_2$ generating formic acid as the major product (with faradaic yield of 70% for the most active and selective one), together with minor amounts of CO and $H_2$. As in the case of the well-studied Ni(cyclam) complex, catalysis occurs exclusively using a Hg electrode. This suggests that Hg contributes to the activation of the catalyst transiently adsorbed at the surface of the electrode. Unexpectedly, significant differences in activity and selectivity are observed between stereoisomers, which also likely results from the interactions between the catalysts and the Hg electrode.

## Introduction

Electroreduction of $CO_2$ into energy-dense organic compounds is extensively studied currently as a way to store intermittent renewable energies in the form of chemical energy durably as well as to use $CO_2$ as a source of carbon in organic synthesis. In order to achieve

high current densities, high energetic efficiencies and high selectivity, necessary for practical applications, stable and cheap catalysts are absolutely required. In particular, molecular catalysts have several substantial benefits, the most specific one residing in the possibility to finely tune their activity and their selectivity by synthetic modification of the ligands.[1, 2]

Recently, realizing that only very few Ni complexes had been explored as catalysts for $CO_2$ electroreduction,[3-7] we initiated a study of a new class of Ni complexes specifically based on bioinspired dithiolene ligands.[8] Indeed, we were intrigued by the fact that, in all natural metalloenzymes catalyzing $CO_2$ reduction, the redox active metal center is coordinated almost exclusively by sulfur atoms. In one class of CO-dehydrogenases, a Ni ion is ligated by two sulfides provided by an iron-sulfur cluster and by one S atom from a cysteine residue while, in formate dehydrogenases, a mononuclear Mo (or W) center is chelated by two molybdopterins, via their bidentate dithiolene moieties.[9, 10] Thanks to the successful synthesis of an original quinoxaline-pyran-fused dithiolene ligand ($qpdt^{2-}$ in Figure 1) inspired by molybdopterin, we reported the first bioinspired Ni(bis-dithiolene) complex, complex **1** (Figure 1), that could perform catalytic electroreduction of $CO_2$ into formate as the major product on a mercury electrode, with remarkable stability, good faradaic yields and reasonable overpotential requirements.[8]

However, the $qpdt^{2-}$ ligand used in this first study had two inter-related drawbacks. First, it is not fully biomimetic since the central pyrazine ring is oxidized while it is fully (tetrahydropyranopterin form) or, sometimes, partially (dihydropyranopterin form) reduced in natural molybdopterin.[11] Second, as a consequence, the imines of the $qpdt^{2-}$ ligand are prone to hydrogenation under reductive conditions in the presence of protons, leading to a further substantial modification of the ligand (specifically the irreversible opening of the pyran ring),[12] so that complex **1** was a pre-catalyst rather than a true catalyst.[8] We have thus recently synthesized two new biomimetic dithiolene ligands, H-qpdt and 2H-qpdt, more biologically relevant to molybdopterin and more stable, both deriving from $qpdt^{2-}$.[13] They are shown in Figure 1 in the protected alkylated forms **2** and **3**, respectively. In H-qpdt one imine is saturated while in 2H-qpdt the two imines are saturated, with a *cis*-configuration for the two H atoms of the ring junction, as it is the case in molybdopterin.

Now we report the synthesis and characterization of Ni complexes, complexes **4** and **5** in Figure 2, based on H-qpdt and 2H-qpdt ligands. We specifically study the chemical and electrochemical hydrogenation of complex **4** and characterize the resulting complexes. Finally, all Ni complexes were characterized for their catalytic properties for the

electroreduction of $CO_2$. The observation of significant differences between stereoisomers in terms of catalytic activity is unexpected and discussed in relation with the important role of the catalyst-mercury interface in promoting catalysis.

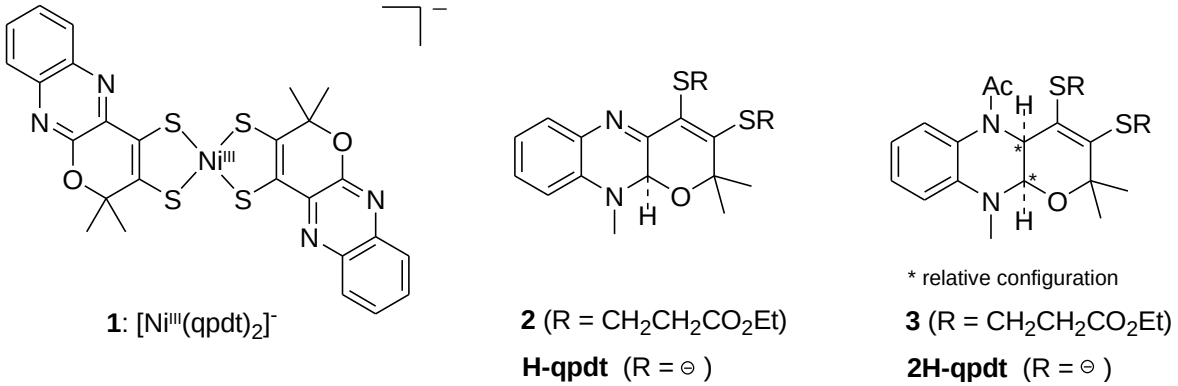


**Figure 1.** Structures of $[Ni^{III}(qpdt)_2]^-$ (complex **1**), H-qpdt and 2H-qpdt ditholene ligands in the protected form **2** and **3**.

## Results

*Synthesis and characterization of Ni(bis-dithiolene) complexes*

The dithiolene ligands of this study were prepared in the protected form (compounds **2** and **3**, Figure 1) as previously described.[13] Compound **2** exists as a mixture of two enantiomers, depending on the configuration, *R* or *S*, of the $sp^3$ carbon at the junction of the central and the pyran rings. Compound **3** has been previously shown to have the two H atoms of the ring junction in a *cis* configuration and thus exists in the form of two enantiomers (*RR* and *SS*).

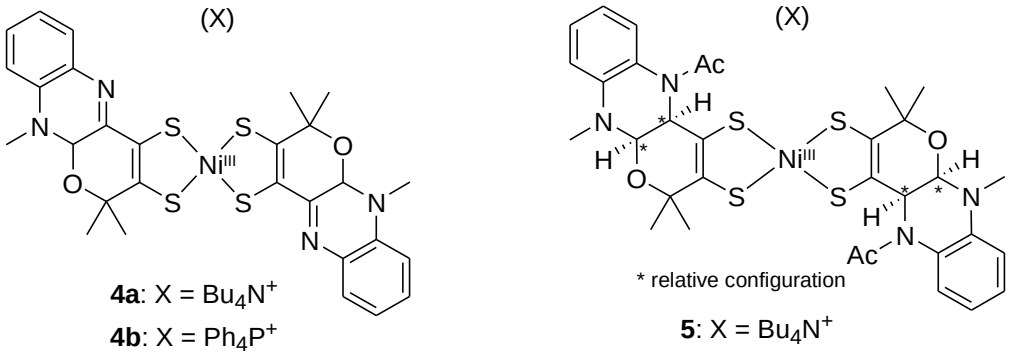

**Figure 2**. Structures of $[Ni^{III}(H\text{-}qpdt)_2]^-$ (**4**) and $[Ni^{III}(2H\text{-}qpdt)_2]^-$ (**5**).

The Ni(bis-dithiolene) complexes **4** and **5** (Figure 2) have been prepared from **2** and **3**, respectively, after deprotection under basic conditions (*t*-BuOK) followed by treatment with $Ni(ClO_4)_2.6H_2O$. After a cation exchange step, two complexes $(Bu_4N)[Ni^{III}(H\text{-}qpdt)_2]$ (**4a**) and $(Ph_4P)[Ni^{III}(H\text{-}qpdt)_2]$ (**4b**) were obtained. However, only **4b** could be crystallized and structurally characterized. A summary of crystal data and refinement parameters are listed in Table S1. Angles and bond lengths given in Table S2 were within the range of values previously reported for Ni(bis-dithiolene) complexes.[14] The molecular structure of the anion component $[Ni^{III}(H\text{-}qpdt)_2]^-$ is shown in Figure 3. The Ni atom is coordinated by four S atoms in a square-planar geometry and the two dithiolene ligands are in *trans*-relationship with a C2 axis of symmetry perpendicular to the $NiS_4$ plane. Since the ligand derived from **2** contains two enantiomers, complex **4** likely exists in the form of three isomers: two enantiomers *trans-RR* and *trans-SS*, as well as the achiral molecule *trans-SR*, with an inversion center positioned on the Ni atom. In the crystal structure of **4b**, the *trans-SR* isomer was found (Figure 3).

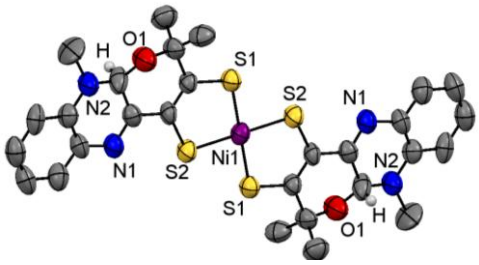


**Figure 3.** ORTEP view of the anion component of $(PPh_4)[Ni^{III}(H\text{-}qpdt)_2]$ (**4b**), some H atoms are omitted for the sake of clarity.

The redox active $Ph_4P^+$ counter-cation is reducible at −1.8 V *vs.* Ag/AgCl,[8] within the range of potentials for catalysis. Thus all $CO_2$ electroreduction experiments were conducted with the same complex having $Bu_4N^+$ as the counter-cation, namely $(Bu_4N)[Ni^{III}(H\text{-}qpdt)_2]$ (**4a**).

For complex **5**, conventional counter-ions ($Et_4N^+$, $Bu_4N^+$ and $Ph_4P^+$) were used for crystallization. Despite many attempts, we failed to obtain single crystals suitable for x-ray diffraction. In the following, **5** is the complex obtained with $Bu_4N^+$ as the counter-ion used throughout the study. Based on UV-vis spectroscopy and mass spectrometry characterization as well as on elemental analysis, complex **5** is proposed to be $(Bu_4N)[Ni^{III}(2H\text{-}qpdt)_2]$ with the structure shown in Figure 2. It is very likely that the two dithiolene ligands are *trans*-oriented,

as in **1** and **4** and as in all Ni(bis-dithiolene) complexes reported previously.[14] Similar to **4**, complex **5** exists in the form of three isomers, *RR-RR*, *SS-SS* and *RR-SS*.

The two complexes **4** and **5** differ from each other with respect to the saturation state of the central ring. This results in differences in terms of physical and chemical properties which are summarized in Table S3. Figure S1 shows the UV/Vis spectra of complexes **4a** and **5** in $CH_3CN$: the characteristic intervalence LLCT band peaks at $\lambda_{max}$ = 955 nm ($\varepsilon$ = 12000 $M^{-1}.cm^{-1}$) for **4a** and at 896 nm ($\varepsilon$ = 9700 $M^{-1}.cm^{-1}$) for **5** with a lower absorbance in the case of **5**, consistent with the ligand in **5** being more electro-donating than in **4**.[15] The redox half wave potential ($E_{p1/2}$) of the Ni(III)/Ni(II) transition thus follows the expected trend as shown by cyclic voltammetry (CV) on a glassy carbon electrode (GCE): an important cathodic shift from **4a** (–0.53 V) to **5** (–0.76 V), potentials reported *vs.* Ag/AgCl, was observed (Figure S2).

Figure 4 presents the CVs in dry $CH_3CN$ on a GCE and a Hg/Au amalgam electrode for both complexes **4a** and **5**. The CVs obtained on the Hg/Au electrode are essentially similar to the ones obtained on GCE (with a reversible Ni(III)/Ni(II) transition between -0.5 V and 0.7 V and an irreversible signal below -2 V likely assigned to a ligand-based process). However only in the case of the Hg/Au electrode tiny additional peaks at –0.95 V for **4a** (Figure 4a) and –0.85 V for **5** (Figure 4b) are observed. A similar behavior has been reported in the case of complex **1**.[8] This is the signature of adsorption of the complexes on the Hg electrode as also reported in the case of the $[Ni(cyclam)]^{2+}$ complex, a well-known catalyst for $CO_2$ electroreduction.[5]

a) b)

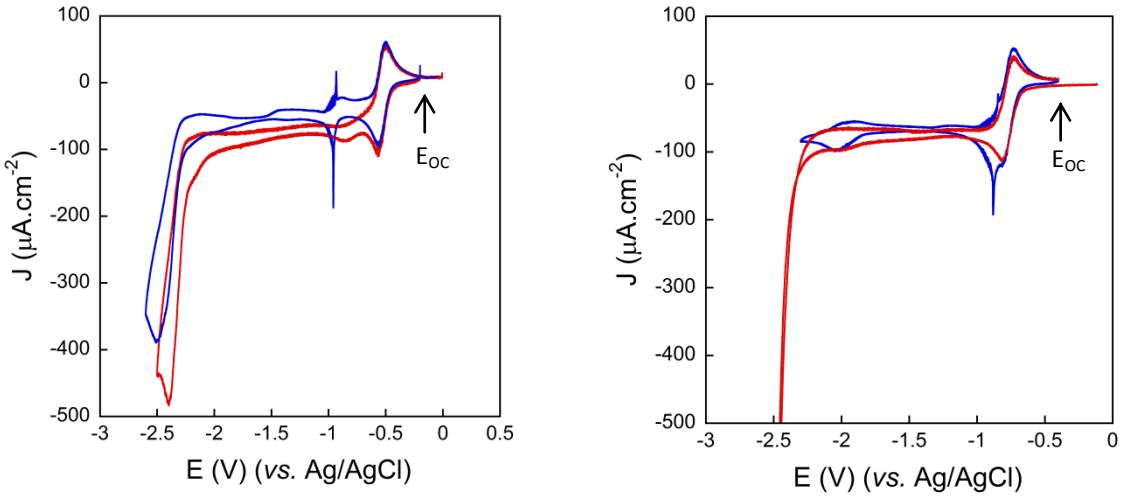


**Figure 4.** Cyclic voltammograms of a) 0.5 mM complex **4a**, b) 0.5 mM complex **5**, 0.1 M tetrabutylammonium perchlorate (TBAP) in dry acetonitrile ($CH_3CN$) under Ar on a GCE (red line) and on a Hg/Au amalgam electrode (blue line). Scan rate: 50 $mV.s^{-1}$; third scan is shown.

*Cyclic Voltammetry of complexes **4** and **5** in the presence of $CO_2$ and a source of protons*

The reduction of $CO_2$ by the two Ni complexes **4a** and **5** was first evaluated by cyclic voltammetry. Complex **1** had been previously shown to behave as a good catalyst for the electroreduction of $CO_2$ in $CH_3CN$ in the presence of a proton source such as trifluoroethanol (TFEH), however exclusively on a Hg electrode and not on a GCE.[8] Thus all the experiments described below have been carried out under similar conditions. Potentials are given *vs.* Ag/AgCl.

As shown in Figures S3 and S4 a catalytic peak appeared for complex **4a** and **5** reaching a maximum at –2 V, however only after addition of $CO_2$ in the presence of TFEH (green lines). No wave can be observed in the absence of acid (blue lines). For both complexes interestingly the Ni(III)/Ni(II) signal shifts anodically by ~ 200 mV, suggesting ligand protonation facilitating electron transfer. Figure 5 shows the redox behaviors of complex **4a** (green line) and **5** (blue line) as well as the CV of a blank solution in the absence of these catalysts (red line) in the presence of $CO_2$ and TFEH for comparison. Complex **4a** exhibits two new irreversible waves at –1.3 V and –1.4 V whereas complex **5** does not. Although both complexes present a similar catalytic wave in terms of onset potential under the same conditions, complex **5** shows much lower intensity.

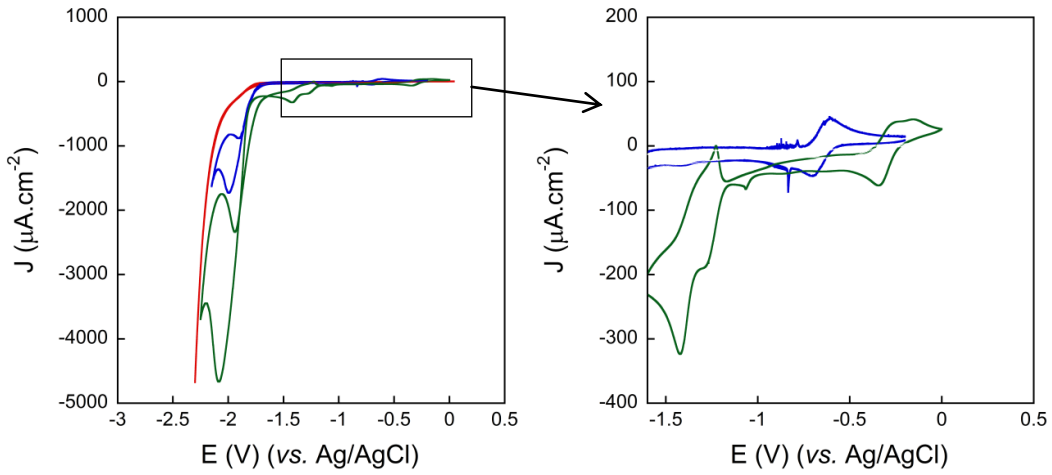


**Figure 5**. Left: Cyclic voltammograms under a $CO_2$ atmosphere in $CH_3CN$, 0.1 M TBAP, 2 M TFEH in the absence of complexes (red line), with 0.5 mM of complex $(Bu_4N)[Ni^{III}(H\text{-}qpdt)_2]$ (**4a**) (green line) and with 0.5 mM of complex $(Bu_4N)[Ni^{III}(2H\text{-}qpdt)_2]$ (**5**) (blue line). Right: Zoom on the redox signals between 0 and –1.5 V. Scan rate 50 $mV.s^{-1}$; Hg/Au amalgam electrode; third scan is shown.

Since only complex **4a** carried ligands containing a reducible imine bond, we assigned the two waves between –1.3 V and –1.4 V to the hydrogenation (proton-coupled reduction) of the imine bond of each dithiolene ligand. Accordingly, these features accounted for a total of 4 electrons (Figure S5). Furthermore, after 4 h electrolysis in a Hg pool electrode of complex **4a**, at –2 V, in the presence of $CO_2$ and TFEH, a new complex, named **6**, was obtained. The UV-visible spectrum (Figure S6a) of the complex showed an intervalence LLCT band at higher energy (930 nm), its CV did not display the redox features at –1.3V and –1.4V and the Ni(III)/Ni(II) redox couple half wave potential shifted cathodically 250 mV (Figure S6b). All these data are consistent with a reduction of the imine moiety of the ligand.

Unfortunately, **6** could not be isolated from the electrolysis mixture for further characterization. We then decided to chemically reduce the imine group of complex **4a** using $NaBH_3CN$ in the presence of acetic acid. After reaction, the reaction product **7** was extracted and recrystallized in $CH_2Cl_2$/pentane. Hydrogenation of the imine groups was confirmed by mass spectrometry and by CV. Indeed, the mass spectrum of **7** displayed a characteristic isotopic pattern at m/z = 642 and the Ni(III)/Ni(II) feature in the CV was cathodically shifted at –0.72 V (Figure S7a). However, the intervalence LLCT band within the UV-Vis spectrum was found at 895 nm, corresponding to a 35 nm hypsochromic shift with respect to **6** (Figure

S7b), indicating that chemical reduction and electrochemical reduction did not result in the same product, **7** was slightly different from **6**. Moreover CVs of complexes **6** and **7** in the presence of $CO_2$ and TFEH displayed important differences (Figure S8). In the case of **6**, catalytic currents are more important and the onset potential has a gain of 200 mV.

*Study of dithiolene ligand reduction using a $Co^{III}Cp$(H-qpdt) complex*

In order to better understand these differences and get insight into the structure of the ligands in complexes **6** and **7**, we used CoCp(dithiolene) complexes, with Cp = cyclopentadienyl, as probes since they are generally very stable and can be purified on solid supports such as alumina or silica. This would ease the isolation of the products formed after chemical and electrochemical reduction. Moreover, they are diamagnetic and can be easily characterized by $^1$H NMR spectroscopy.[16]

Synthesis and characterization of the starting **[**$Co^{III}$Cp(H-qpdt)] complex (**8** shown in Scheme 1) has been recently reported.[13] Complex **8** was first treated with $NaBH_3CN$ in the presence of acetic acid in $CH_3CN$ and the resulting stable complex **9** was isolated and characterized by mass spectrometry and NMR spectroscopy (Figure S9a). The data clearly showed that **9** had its imine function indeed fully hydrogenated. In particular the weak coupling constant ($J$ = 1.7 Hz) between the two newly introduced H atoms (doublets at 4.4 and 4.9 ppm in the NMR spectrum, Figure S9c) and a NOE 1D experiment clearly established a *cis* relative stereochemistry for the 2 H atoms (scheme 1).

Complex **8** was also electrochemically reduced through bulk electrolysis in $CH_3CN$ in the presence of TFEH and $CO_2$ at –1.5 V *vs.* Ag/AgCl. These conditions were defined on the basis of the information provided by CV of complex **8**. Indeed, exclusively after addition of TFEH, a new irreversible redox wave appeared at –1.39 V, accounting for 2 electrons and assigned to the reduction of the imine of the ligand (Figure S10). Surprisingly, the outcome of the reaction depended on the type of working electrode used for electrolysis: when the electrolysis was carried out on a GCE, the product of the reaction was identical to **9** while on a Hg pool, a new complex **10** was obtained. Mass spectrometry and NMR spectroscopy (Figure S9b) of the isolated product **10** allowed us to establish that the imine group was also fully hydrogenated. However, the NMR spectrum was different from that of **9**, especially for the newly introduced H atoms (Figure S9c). The two protons were found at 3.5 and 4.2 ppm and were strongly coupled ($J$ = 6.9 Hz). This together with a NOE 1D experiment established

that these two H atoms are in a *trans* configuration. The structures of **9** and **10** are shown in Scheme 1. Hydrogenation of the central ring in **9** and **10** was reflected in the Co(III)/Co(II) redox potential (**9**: –0.72 V ; **10**: –0.69 V *vs.* Ag/AgCl), cathodically shifted with respect to **8** (Table S3).

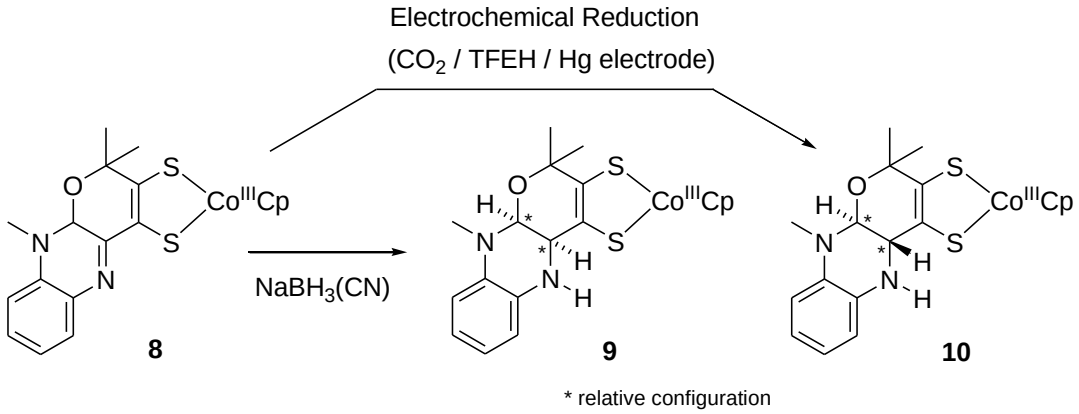


**Scheme 1.** Chemical and electrochemical reduction of **8** leading to different cycle junctions.

In conclusion, chemical reduction of the H-qpdt ligand within complex **8** introduces the two H atoms in a *cis* configuration while electrochemical reduction on a Hg electrode results in a *trans* configuration. We propose that the same occurs with the Ni complex **4a** and that the configuration at the ring junction is different in **6** and **7**, likely *trans* and *cis* respectively (Figure 6)**.**

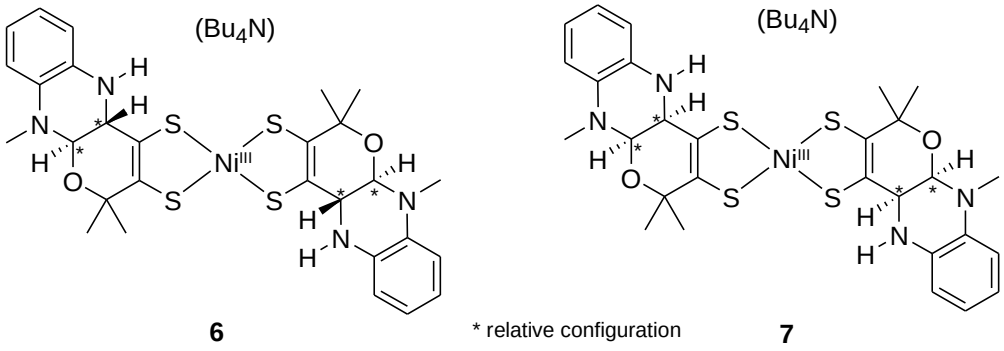


**Figure 6.** Structures of complexes **6** and **7** obtained by electrochemical reduction (on a Hg electrode) and chemical reduction of **4a**, respectively.

*Catalytic electroreduction of $CO_2$ studied by controlled potential electrolysis*

We investigated the different Ni complexes with fully reduced dithiolene ligands, namely complexes **5**, **6** and **7**, but did not consider complex **4a** since under the electrochemical reductive conditions of the catalytic reaction **4a** is converted to **6** as described above.

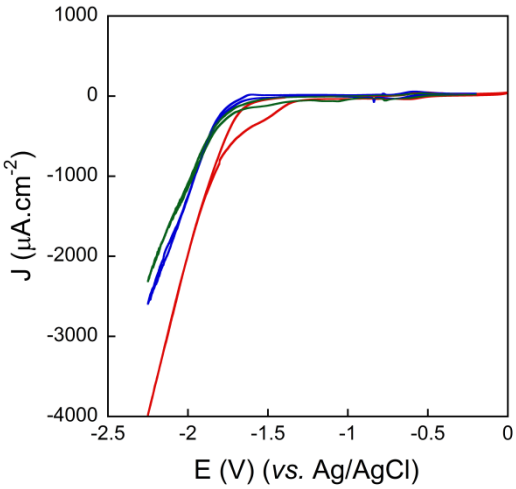


**Figure 7.** Cyclic voltammograms under a $CO_2$ atmosphere in $CH_3CN$, 0.1 M TBAP, 2 M TFEH with 0.5 mM of complex **5** (blue line), 0.5 mM of complex **6** (red line) and 0.5 mM of complex **7** (green line). Scan rate 50 $mV.s^{-1}$; Hg pool electrode; third scans are shown.

Figure 7 shows the CV of the three complexes in $CO_2$ saturated $CH_3CN$ in the presence of 0.1 M TBAP and 2 M TFEH. In all cases, a catalytic wave was observed, with **6** displaying the largest activity (largest current density for a given potential) and **5** and **7** behaving similarly. Based on onset potentials and the value of –1.36 V *vs.* $Ag/AgCl/KCl_{sat}$ for $E^0_{CH3CN}$ ($CO_2$/HCOOH, TFEH), calculated previously,[8] and used here since formate was the major reduction product, onset overpotential of ~ 500 mV, 300 mV and 480 mV were estimated for **5**, **6** and **7** during 4 hours respectively.

Controlled potential electrolysis (CPE) was carried out at –2.0 V during 4 hours. In all cases, the current densities were stable during the duration of the electrolysis (Figure S11). The gaseous products, $H_2$ and CO, were quantified by gas chromatography and formic acid by ion-exchange liquid chromatography. No other products could be detected. No CO and formic acid could be detected when the electrolysis was carried out in the absence of $CO_2$.

As expected from the CV data, complex **6** gave the largest total TON value, in agreement with **6** being the most active catalyst (Figure 8). In addition, while in all cases, formate was the major reaction product (Figure 8 and Table S4), complex **6** was by far the most selective catalyst for $CO_2$ reduction (Faradaic Yield (FY) of 82%) over $H^+$ reduction (FY= 4%) and in addition more selective for formic acid formation than for CO formation (FY= 70% and 12%, respectively). Slight differences were also observed between **5** and **7**, since **5** was more selective for formic acid formation (FY= 53% for **5** and 35% for **7**) while **7** gave a much larger proportion of $H_2$ (FY= 8% for **5** and 19% for **7**). The three complexes were quite stable since, after 4 h of electrolysis at –2.0 V, the peak potentials of the $Ni^{III}/Ni^{II}$ wave in CVs are unchanged and the intensity only slightly diminished (Figure S12).

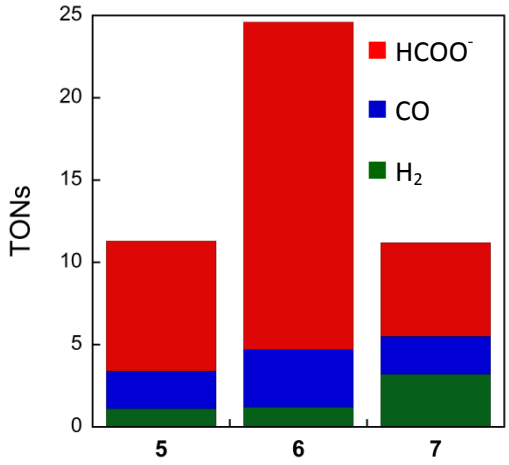


**Figure 8.** TONs of formate (■), CO (■) and $H_2$ (■) after 4 hours of electrolysis at –2.0 V on a Hg pool electrode. Each sample contains 0.5 mM of catalyst (**5**, **6** or **7**), 2 M of TFEH and 0.1 M of TBAP in $CO_2$-saturated $CH_3CN$. TONs are based on the catalyst bulk concentration.

A longer CPE experiment (20 h) was carried out with complex **6**. The current density was quite stable over this time with only a 30% loss at the end of the experiment (Figure S13a) and UV-vis spectroscopic and CV characterization (Figures S13b and S13c) showed the presence of complex **6** in the solution. After 20 h electrolysis, an important amount of formate (70 TONs, 56% faradic yield) was formed, together with CO (19.6 TONs, 16%) and $H_2$ (7.7 TONs, 6%).

**Discussion**

Expanding the class of bioinspired Ni(bis-dithiolene) catalysts for $CO_2$ electroreduction has led to three new complexes based on molybdopterin-like dithiolene ligands, namely complexes **5**, **6** and **7**. In all three complexes, as in formate dehydrogenases, the central

pyrazine ring is fully saturated and thus cannot be further modified during catalysis. As a consequence, in contrast to the only previously reported example of a functional Ni(bis-dithiolene) catalyst, namely complex **1**,[8] the new complexes reported here are structurally stable under the reductive conditions of the reaction ~~and behave as true catalysts and not precatalysts~~. This provides a strong basis for a structure-activity relationship study.

As an interesting outcome of the study, we report here a new catalyst, complex **6**, with much greater activity and selectivity than the previously reported related complex **1**. At comparable applied potentials, complex **6** achieves almost 25 total TONs in 4 hours, with a FY for formic acid of 70%, whereas complex **1** achieves 13 TONs in 4 hours, with a FY for formic acid of 60 %. In particular, complex **6** generates very little $H_2$ (FY= 4%), greatly favoring $CO_2$ reduction over $H^+$ reduction (Figure 8). Thus complex **6** is so far the best catalyst of this class and complexes **1**, **5** and **7** display comparable activities with slight differences in selectivity, with formic acid being the major product in all cases.

The most intriguing observation is the great difference between complexes **6** and **7** in terms of activity and selectivity (Figure 8). Indeed, the two complexes are structurally very similar (Figure 6), the only difference residing in the configuration of the ring junction, a difference which was obviously not expected to be reflected in the respective catalytic activity. It is very likely that this is the consequence of using a working electrode of Hg which clearly provides to the active catalyst a specific environment responsible for the stimulation of the catalytic activity and most probably for the tuning of the selectivity. Indeed, herein we show that the complexes adsorb at the surface of the Hg electrode and their catalytic activity is dramatically enhanced on such an electrode as compared to a standard GCE, thus suggesting that the active species is slightly different from the homogeneous complex. There is a famous example, extensively studied recently by Kubiak and co-workers, of a Ni catalyst for $CO_2$ electroreduction, namely $[Ni(cyclam)]^{2+}$, behaving similarly.[17, 18] In that specific case, it has been proposed that the increase of catalytic activity was due to favorable noncovalent interactions between the cyclam ligand and the surface of the Hg electrode leading to the adsorption of the most active conformer, favoring $CO_2$ binding and facilitating desorption of CO, a poison of the catalyst.[19, 20] Even though this hypothesis needs to be studied specifically, we believe that similar scenarios are at work in the case of the Ni(bis-dithiolene) complexes studied here, in which noncovalent interactions between the dithiolene ligands and the Hg surface differentiate between stereoisomers. Better understanding of the

structure of the adsorbed active species, unfortunately challenging, might open perspectives for improving catalyst performances.

## Experimental Section

### General methods

All starting materials were commercially available (Sigma and Acros) and were used without further purification. Solvents were purified by an MBRAUN SPS-800 Solvent Purification System. All reactions were carried out under air atmosphere unless specified. $^{1}H$ and $^{13}C$ NMR spectra were recorded on a Bruker Avance-III 300 NMR spectrometer (300 MHz for $^{1}H$, 75 MHz for $^{13}C$) at room temperature. High-resolution mass spectra (HRMS) were recorded on a LCT Premier XE mass spectrometer using ESI (electrospray ionization) at Institut de Chimie des Substances Naturelles in Gif-sur-Yvette. Mass spectra (MS) were recorded on an Applied Biosystems QSTAR pulsar I mass spectrometer using ESI (electrospray ionization) at Museum National d'Histoire Naturelle (Paris). Flash chromatography was performed on Grace Reverlis® x2 with corresponding cartridges. UV-Vis spectra were recorded using a Cary 100 UV-Vis spectrophotometer instrument (Agilent).

### Electrochemical experiments

All cyclic voltammetry (CVs) experiments were performed in a conventional three-electrode single-compartment cell with a SP 300 Bio-Logic potentiostat (Bio-Logic Science Instruments SAS). A saturated Ag/AgCl/KCl electrode (hereafter abbreviated as Ag/AgCl) was placed in the same compartment as the working electrode separated by a bridge with a Vycor frit and was used as the reference electrode. A platinum counter electrode was separated from the solution by a glass frit. Glassy carbon electrode (BASi) of 1 mm diameter, a Hg/Au amalgam electrode or a Hg pool of 1.17 $cm^2$ were used as working electrodes. The Hg/Au amalgam electrode was prepared by dipping a 1.6 mm diameter Au disk electrode (BASi) into a pool of mercury. The electrochemical area was determined by using an internal reference (in this case complex **4a**) and comparing the current intensity of the Ni(III)/Ni(II) redox couple to the one obtained with a GCE (known area). It was calculated to be 2.68 $mm^2$. The disk electrodes were polished on wet polishing cloth using a 1 µm diamond suspension and a 0.05 µm alumina slurry. The scan rate was 50 $mV.s^{-1}$. Solutions of dry acetonitrile ($CH_3CN$) containing 0.1 M tetrabutylammonium perchlorate (TBAP) as the supporting electrolyte were bulk deaerated with Ar or $CO_2$ for at least 15 min before CVs.

Bulk electrolysis experiments were carried out at room temperature in a custom-built, gas-tight two-compartment electrochemical cell specific for mercury that has been previously described.[8] The cathodic and anodic compartments are separated via a porous glass frit of fine porosity. Bulk solutions, constantly stirred, of 0.5 mM of catalysts and 2 M of trifluoroethanol (TFEH) in acetonitrile containing 0.1 M TBAP were purged with $CO_2$ gas for 30 min before starting the experiment. The working electrode was a pool of 0.5 mL of mercury, the counter electrode was a 0.5 mm diameter platinum wire and the reference electrode was a saturated Ag/AgCl/KCl electrode. Carbon monoxide was detected with a gas chromatograph (Shimadzu GC-2010) equipped with a methanizer, a flame induction detector (FID), and a shincarbon ST (Restek) column. Hydrogen was detected a gas chromatograph coupled to a thermal conductivity detector (Shimadzu GC-2014). Aliquots of gas were removed with a gas-tight syringe. Formic acid concentrations were determined by ionic exchange liquid chromatography (883 Basic IC, Metrohm).

Due to its toxicity, mercury should be manipulated under the fume hood which is exclusively used for these experiments. The Material Safety Data Sheet (MSDS) should be kept next to the fume hood.

**Synthesis of complexes**

**Synthesis of $(Bu_4N)[Ni^{III}(H\text{-}qpdt)_2]$ (4a).** The experiment was carried out under Ar using Schlenk tube and all solutions were degassed prior to use. *t*BuOK (52 mg, 0.46 mmol) was added to a solution of **2** (57 mg, 0.12 mmol) in anhydrous THF (2 mL) at 0°C. After 30 min at room temperature, a solution of $Ni(ClO_4)_2.6H_2O$ (22 mg, 0.06 mmol) in MeOH (2 mL) was added dropwise via a cannula needle to the orange suspension. An immediate color change to brown-red was observed. After 2 h, the reaction was exposed to air and an aqueous solution of $Bu_4NBr$ (60 mg, 0.19 mmol) was added (5 mL). The precipitate was filtered, rinsed with water and vacuum dried. The crude product was purified by slow diffusion of $Et_2O$ into its THF solution to afford **4a** as a brown solid (22 mg, 43%). UV-Vis ($CH_3CN$), $\lambda_{max}$ nm ($\varepsilon$ $M^{-1}.cm^{-1}$): 955 (12000), 567 (3000), 480 (3300), 382 (27000), 312 (26800). Negative-ion Electrospray MS ($CH_3CN$) *m/z*: 638 $[Ni^{III}(H\text{-}qpdt)_2]^-$. *Anal.* Calc. for $C_{48}H_{77}N_5NiO_6S_4$ (**4a**. $3(H_2O)$.THF, 1005,4110): C 57.25, H 7.71, N 6.95, S 12.73; Found: C 57.39, H 7.30, N 7.01, S 12.74.

**($Ph_4P$)[$Ni^{III}$(H-qpdt)$_2$] (4b)** was synthesized by the same procedure as for **4a**, except that $Ph_4PCl$ was used instead of $Bu_4NBr$ (yield 52%). Single crystals suitable for X-ray diffraction were obtained by layering pentane over a solution of $CH_2Cl_2$ containing **4b** at room temperature.

**Synthesis of ($Bu_4N$)[$Ni^{III}$(2H-qpdt)$_2$] (5).** This complex was synthesized according to the same procedure as for complex **4a**, with *t*BuOK (116 mg, 1.04 mmol), **3** (139 mg, 0.26 mmol), $Ni(ClO_4)_2.6H_2O$ (48 mg, 0.13 mmol) and $Bu_4NBr$ (84 mg, 0.26 mmol). The crude product was purified in a glove box by slow diffusion of $Et_2O$ into its $CH_3CN$ solution to afford **5** as a pale purple solid (56 mg, 45%). UV-Vis ($CH_3CN$), $\lambda_{max}$ nm ($\varepsilon$ $M^{-1}.cm^{-1}$): 896 (9700), 536 (1300), 355 (5000), 307 (22400). Negative-ion Electrospray MS ($CH_3CN$) *m/z*: 726 [$Ni^{III}$(2H-qpdt)$_2$]$^-$. *Anal.* Calc. for $C_{96}H_{154}N_{10}Ni_2O_{13}S_8$ (2 **5**.5($H_2O$), 2026.8392): C 56.79, H 7.65, N 6.90, S 12.63; Found: C 56.71, H 7.11, N 6.52, S 12.15.

**5** was conserved in a glove box, since it slowly oxidized in air.

**Synthesis of complex 9 by chemical reduction of [$Co^{III}$Cp(H-qpdt)] (8).** Under an Ar atmosphere, AcOH (10 $\mu$L, 0.16 mmol) and $NaBH_3CN$ (7 mg, 0.11 mmol) were added to a solution of **8** (22 mg, 0.05 mmol) in dry $CH_2Cl_2$ (3 mL) and $CH_3CN$ (3 mL) cooled to 0 °C. The blue-green solution was kept at room temperature overnight, and the color of the solution turned to purple. The reaction mixture was treated with a saturated aqueous solution of $NaHCO_3$ and the usual work-up with $CH_2Cl_2$ gave 9 as a purple powder, which was directly used without further purification. UV-Vis ($CH_3CN$), $\lambda_{max}$ nm ($\varepsilon$ $M^{-1}.cm^{-1}$): 720 (500), 569 (7600), 414 (1600), 283 (22000). Positive-ion Electrospray MS (MeOH) *m/z*: 417 $[M + H]^+$. $^1H$ NMR (300 MHz, $CDCl_3$) $\delta$ 6.76 – 6.68 (m, 1H), 6.60 (m, 2H), 6.52 (dd, $J$ = 7.9, 1.5 Hz, 1H), 5.37 (s, 5H), 4.83 (d, $J$ = 1.8 Hz, 1H), 4.40 (d, $J$ = 1.8 Hz, 1H), 3.02 (s, 3H), 1.67 (d, $J$ = 7.5 Hz, 6H).

**Synthesis of complex 10 by electrochemical reduction of [$Co^{III}$Cp(H-qpdt)] (8).** Trifluoroethanol (1.58 mL, 22 mmol) was added to a solution of **8** (9 mg, 0.022 mmol) in anhydrous $CH_3CN$ (11 mL) containing tetrabutylammonium perchlorate (0.1 M). The solution was purged with $CO_2$ gas for 30 min before electrolysis and was constantly stirred. The controlled-potential electrolysis was carried out at –2.0 V *vs.* Ag/AgCl/KCl (sat) with a Hg electrode ($\phi$ = 10 mm). The reaction was monitored by cyclic voltammetry (CV) until the disappearance of $E_{rev}(Co^{III}/Co^{II})$ at –0.59 V (*vs.* $Ag/AgCl/KCl_{sat}$). After evaporation of the solvent, $Et_2O$ was added and the suspension was centrifuged. The supernatant was concentrated in *vacuo* and purified by flash chromatography over alumina (eluting with AcOEt/cyclohexane, 1:9) to afford **9** as a deep-blue solid (4 mg, 42 %). UV-Vis ($CH_3CN$), $\lambda_{max}$ nm ($\varepsilon$ $M^{-1}.cm^{-1}$): 730 (500), 581 (5800), 407 (1600), 283 (17000). Positive-ion Electrospray MS (MeOH) *m/z*: 417 $[M + H]^+$. $^1H$ NMR (300 MHz, $CDCl_3$) $\delta$ 6.82 (d, $J$ = 7.7 Hz, 1H), 6.79 – 6.71 (m, 2H), 6.71 – 6.64 (m, 1H), 5.48 (s, 5H), 5.04 (s, 1H), 4.18 (d, $J$ = 6.9 Hz, 1H), 3.54 (dd, $J$ = 6.9, 1.4 Hz, 1H), 2.89 (s, 3H), 1.74 (s, 3H), 1.67 (s, 3H).

**Synthesis of complex 7 by chemical reduction of $(Bu_4N)[Ni^{III}(H\text{-}qpdt)_2]$ (4a).** Under an Ar atmosphere, AcOH (7 $\mu$L, 0.13 mmol) and $NaBH_3CN$ (11 mg, 0.17 mmol) were added to a degassed solution of **4a** (37 mg, 0.04 mmol) in dry $CH_3CN$ (5 mL) cooled to 0 °C. The brown solution was kept at room temperature overnight, and the color of the solution turned to purple. The reaction mixture was treated with a saturated aqueous solution of $NaHCO_3$ and the usual work-up with $CH_2Cl_2$ gave a crude product which was purified by precipitation in $CH_3CN/Et_2O$ to yield **7** as a purple powder (29 mg, 73%). UV-Vis ($CH_3CN$), $\lambda_{max}$ nm ($\varepsilon$ $M^{-1}.cm^{-1}$): 895 (8200), 633 (sh), 514 (1400), 366 (6900), 311 (25000). Negative-ion Electrospray MS ($CH_3CN$) *m/z*: 642 $[M]^-$.

**7** was conserved in a glove box, since it slowly oxidized in air.

## ASSOCIATED CONTENT

### Supporting Information

The Supporting Information (figures of electrochemistry study, NMR spectra, tables and X-ray crystallographic data) is available free of charge on the ACS Publications website at http://pubs.acs.org.

The authors declare no competing financial interests.

## ACKNOWLEDGEMENTS

We acknowledge support from the French National Research Agency (ANR, PhotoCarb ANR-16-CE05-0025-01; Grant "Labex DYNAMO" ANR-11-LABX-0011).

## References

(1) Elgrishi, N.; Chambers, M. B.; Wang, X.; Fontecave, M., Molecular polypyridine-based metal complexes as catalysts for the reduction of $CO_2$, *Chem. Soc. Rev.* **2017,** *46*(3), 761-796.

(2) Takeda, H.; Cometto, C.; Ishitani, O.; Robert, M., Electrons, Photons, Protons and Earth-Abundant Metal Complexes for Molecular Catalysis of $CO_2$ Reduction, *ACS Catal.* **2017,** *7(1)*, 70-88.

(3) Beley, M.; Collin, J. P.; Ruppert, R.; Sauvage, J. P., Electrocatalytic reduction of carbon dioxide by nickel cyclam$^{2+}$ in water: study of the factors affecting the efficiency and the selectivity of the process, *J. Am. Chem. Soc.* **1986,** *108(24)*, 7461-7467.

(4) Beley, M.; Collin, J.-P.; Ruppert, R.; Sauvage, J.-P., Nickel (II)-cyclam: an extremely selective electrocatalyst for reduction of $CO_2$ in water, *J. Chem. Soc., Chem. Commun.* **1984**, (19), 1315-1316.

(5) Collin, J. P.; Jouaiti, A.; Sauvage, J. P., Electrocatalytic properties of Ni(cyclam)$^{2+}$ and $Ni_2$(biscyclam)$^{4+}$ with respect to carbon dioxide and water reduction, *Inorg. Chem.* **1988,** *27(11)*, 1986-1990.

(6) Fisher, B. J.; Eisenberg, R., Electrocatalytic reduction of carbon dioxide by using macrocycles of nickel and cobalt, *J. Am. Chem. Soc.* **1980,** *102(24)*, 7361-7363.

(7) Kuehnel, M. F.; Orchard, K. L.; Dalle, K. E.; Reisner, E., Selective Photocatalytic $CO_2$ Reduction in Water through Anchoring of a Molecular Ni Catalyst on CdS Nanocrystals, *J. Am. Chem. Soc.* **2017,** *139(21)*, 7217-7223.

(8) Fogeron, T.; Todorova, T. K.; Porcher, J. P.; Gomez-Mingot, M.; Chamoreau, L. M.; Mellot-Draznieks, C.; Li, Y.; Fontecave, M., A Bioinspired Nickel(bis-dithiolene) Complex as a Homogeneous Catalyst for Carbon Dioxide Electroreduction, *ACS Catal.* **2018,** *8(3)*, 2030-2038.

(9) Romao, M. J., Molybdenum and tungsten enzymes: a crystallographic and mechanistic overview, *Dalton Trans.* **2009**, (21), 4053-4068.

(10) Maia, L. B.; Moura, J. J. G.; Moura, I., Molybdenum and tungsten-dependent formate dehydrogenases, *J. Biol. Inorg. Chem.* **2015,** *20(2)*, 287-309.

(11) Adamson, H.; Simonov, A. N.; Kierzek, M.; Rothery, R. A.; Weiner, J. H.; Bond, A. M.; Parkin, A., Electrochemical evidence that pyranopterin redox chemistry controls the catalysis of YedY, a mononuclear Mo enzyme, *PNAS* **2015,** *112(47)*, 14506-14511.

(12) Fogeron, T.; Retailleau, P.; Chamoreau, L. M.; Fontecave, M.; Li, Y., The unusual ring scission of a quinoxaline-pyranfused dithiolene system related to molybdopterin, *Dalton Trans.* **2017,** *46(13)*, 4161-4164.

(13) Fogeron, T.; Retailleau, P.; Chamoreau, L.-M.; Li, Y.; Fontecave, M., Pyranopterin Related Dithiolene Molybdenum Complexes as Homogeneous Catalysts for $CO_2$ Photoreduction , submitted.

(14) Zarkadoulas, A.; Field, M. J.; Papatriantafyllopoulou, C.; Fize, J.; Artero, V.; Mitsopoulou, C. A., Experimental and Theoretical Insight into Electrocatalytic Hydrogen Evolution with Nickel Bis(aryldithiolene) Complexes as Catalysts, *Inorg. Chem.* **2016,** *55(2)*, 432-444.

(15). Ray, K.; Weyhermuller, T.; Neese, F.; Wieghardt, K., Electronic structure of square planar bis(benzene-1,2-dithiolato)metal complexes [M(L)(2)](z) (z = 2-, 1-, 0; M = Ni, Pd, Pt, Cu, Au): an experimental, density functional, and correlated ab initio study, *Inorg. Chem.* **2005,** *44*, 5345-60.

(16) Alphonse, F. A.; Karim, R.; Cano-Soumillac, C.; Hebray, M.; Collison, D.; Garner, C. D.; Joule, J. A., A bis($\eta^5$-cyclopentadienyl)cobalt complex of a bis-dithiolene: a chemical analogue of the metal centres of the DMSO reductase family of molybdenum and tungsten

enzymes, in particular ferredoxin aldehyde oxidoreductase, *Tetrahedron* **2005,** *61(46)*, 11010-11019.

(17) Froehlich, J. D.; Kubiak, C. P., Homogeneous $CO_2$ Reduction by Ni(cyclam) at a Glassy Carbon Electrode, *Inorg. Chem.* **2012,** *51(7)*, 3932-3934.

(18) Schneider, J.; Jia, H. F.; Kobiro, K.; Cabelli, D. E.; Muckerman, J. T.; Fujita, E., Nickel(II) macrocycles: highly efficient electrocatalysts for the selective reduction of $CO_2$ to CO, *Energy Environ. Sci.* **2012,** *5(11)*, 9502-9510.

(19) Froehlich, J. D.; Kubiak, C. P., The homogeneous reduction of $CO_2$ by $[Ni(cyclam)]^+$: increased catalytic rates with the addition of a CO scavenger, *J. Am. Chem. Soc.* **2015,** *137(10)*, 3565-73.

(20) Wu, Y.; Rudshteyn, B.; Zhanaidarova, A.; Froehlich, J. D.; Ding, W.; Kubiak, C. P.; Batista, V. S., Electrode-Ligand Interactions Dramatically Enhance $CO_2$ Conversion to CO by the $[Ni(cyclam)](PF_6)_2$ Catalyst, *ACS Catal.* **2017,** *7(8)*, 5282-5288.